Three-Dimensional Description of the Spontaneous Onset of Homochirality on the Surface of a Conglomerate Crystal Phase

Raphaël Plasson,* Dilip K. Kondepudi,† and Kouichi Asakura

Department of Applied Chemistry, Faculty of Sciences and Technology, Keio University, 3-14-1, Hiyoshi, Kohoku-ku, Yokohama, 223-8522, Japan

Received: December 26, 2005; In Final Form: March 11, 2006

The spontaneous emergence of homochirality in an initially racemic system can be obtained in far-from-equilibrium states. Traditional models do not take into account the influence of inhomogeneities, while they may be of great importance. What would happen when one configuration emerges at one position, and the opposite one at another position? We present a discrete three-dimensional model of conglomerate crystallization, based on 1,1′-binaphthyl crystallization experiments, that takes into account the position and environment of every single elementary growth subunit. Stochastic simulations were performed to predict the evolution of the crystallization process. It is shown that the traditional view of the symmetry breaking can then be extended. Fluctuations of the fixed points related to inhomogeneities are observed, and complex behavior, such as local instabilities, transient structures, and chaotic behavior, can emerge. Our modeling indicates that such complex phenomena could cause large fluctuation of the final enantiomeric excess that is observed experimentally in binaphthyl crystallization. The results presented in this article show the importance of inhomogeneities in understanding enantiomeric excess generated in crystallization and the inadequacy of the models based on the assumption of homogeneity.

Introduction

The onset of homochirality, a well-known key element in the understanding of the origin of life, has become an important fundamental field in physical chemistry.[1] This subject is particularly appealing as part of the philosophical question of the meaning of symmetry in nature. How can asymmetry originate spontaneously in a symmetrical environment without contradicting the Curie's principle[2]—which states that effects have asymmetry of the causes that generated the effects? While the racemic states is always the only stable one at equilibrium, stable homochiral states can be maintained in far-from-equilibrium systems, through the flow of matter and energy, as it actually occurs in living beings.

Kondepudi and Nelson[3] developed a theoretical model, on the basis of the early Frank's model.[4] It explains how chiral symmetry breaking can occur in a totally symmetrical system. The system is maintained out of equilibrium by an inflow of reactants and an outflow of products. The presence of nonlinear autocatalytic reactions allows—for a given set of parameters—the destabilization of the symmetric racemic state and the stabilization of asymmetric nonracemic states, each the mirror image of the other; the set of asymmetric solutions transforms into itself under reflection. As a consequence, these systems spontaneously evolve toward nonracemic states.

Several experimental systems showing such a symmetry breaking behavior have been reported so far. Some of them are based on conglomerate crystallization in stirred crystallization, in particular $NaClO_3$ [5] or 1,1′-binaphthyl crystallization.[6] In these cases, the autocatalytic behavior is provided by secondary nucleation of homochiral crystals from an initial seed:[7] each crystal favors the formation of a new elementary growth subunit of the same enantiomer. In the field of prebiotic chemistry, a theoretical framework based on experimental data was recently described,[8] explaining how such a symmetry breaking behavior can be observed in a simple system of polymerization/depolymerization of amino acids.

A major drawback of these models is that they describe homogeneous systems. The presence of inhomogeneities may, however, be important, as it can influence the local structure formation that in turn influences the global behavior[9] in nonequilibrium systems. One may, for example, wonder what would happen when one configuration emerges at one position in the system, and the opposite one at another position. This point is of great importance in prebiotic chemistry for the relevance of far-from-equilibrium systems in the description of the emergence of a unique chirality on the whole Earth. However, only a few simplified models were developed to address this issue.[10] They describe how one unique chirality can globally dominate in a nonhomogeneous Frank-like model thanks to diffusion of compounds.

The work presented here develops a theoretical nonhomogeneous model, based on experimental systems. The conglomerate crystallization of 1,1′-binaphthyl was taken for such a model. Indeed, experiments show that deviations exist from the simple theoretical homogeneous model: one crystal may not grow in a single monocrystalline homochiral block, but is rather composed of several homochiral smaller crystallites. All these crystallites may not be of the same configuration, leading to a partially homochiral system, with enantiomeric excesses of about 60%. Moreover, huge fluctuations of final ee were observed in experiments.[6]

A theoretical kinetic model was developed to explain the observed chiral symmetry breaking[11] according to the surface

* Address correspondence to this author. E-mail: plasson@educ.cc.keio.ac.jp.

† Current address: Department of Chemistry, Wake Forest University, Winston-Salem, NC 27109.

10.1021/jp057511y CCC: $33.50
Published on Web 04/05/2006

SCHEME 1: Homogeneous Kinetic Model of the Growth Front of Conglomerate Crystal Phase[a]

$$L + I_S \xrightarrow{k_{01}} G_S + C_S$$
$$L + I_R \xrightarrow{k_{01}} G_R + C_R$$
$$L + I_S \xrightarrow{k_{02}} G_R + C_S$$
$$L + I_R \xrightarrow{k_{02}} G_S + C_R$$
$$L + I_S + G_S \xrightarrow{k_{11}} G_S + C_S + G_S$$
$$L + I_R + G_R \xrightarrow{k_{11}} G_R + C_R + G_R$$
$$L + I_S + G_R \xrightarrow{k_{12}} G_S + C_S + G_R$$
$$L + I_S + G_R \xrightarrow{k_{12}} G_R + C_S + G_R$$
$$L + I_R + G_S \xrightarrow{k_{12}} G_S + C_R + G_S$$
$$L + I_R + G_S \xrightarrow{k_{12}} G_R + C_R + G_S$$
$$L + I_S + G_S \xrightarrow{k_{13}} G_R + C_S + G_S$$
$$L + I_R + G_R \xrightarrow{k_{13}} G_S + C_R + G_R$$
$$G_S \xrightarrow{k_{20}} I_S$$
$$G_R \xrightarrow{k_{20}} I_R$$

[a] L: liquid phase. G_S, G_R: growth layer. I_S, I_R: interface of crystal to liquid. C_S, C_R: crystal bulk phase.

nucleation growth model[12] of the crystal surface. The surface is seen as a moving open system (the crystallization front) with the inflow of the liquid phase that is to be crystallized and the outflow of the newly formed crystal phase. When the liquid phase (L) goes in contact with the crystal interface (I), it can be integrated to a growth unit (G). The configuration of this new crystalline phase will depend on the configuration of the interface site. It eventually can also be catalyzed by the configuration of the growth unit. The growth unit is afterward converted to an interfacial crystal unit. All these kinetic steps are detailed in Scheme 1.

This set of kinetic equations based on this model succeeded in describing the crystal growth process as an open system, presenting symmetry breaking behavior toward homochirality.[11] However, this theoretical framework gave nearly 100% ee whereas the experimental data of binaphthyl crystallization often gave a value in the 60−70% range. In addition, the approximations made in the model lead to a discontinuous "hard transition" between the symmetric and the asymmetric states, rather than the classical continuous bifurcation diagram, that resembles a second-order phase transition. Second, experiments show intrinsic fluctuations of the final ee between several consecutive experiments, which cannot be understood with this model.

So, what happens in the crystallization of binaphthyls? A first approach would be to consider that multiple seeding of crystals of both R and S configuration occurs, resulting in low enantiomeric excess. However, binaphthyl crystallization is a very slow process, generally taking several days for the crystals to form. The limiting kinetic factor is the formation of a first nucleus; the subsequent growth of the crystal takes place in a few hours. Thus, only one initial nucleation generally occurs, and the whole crystal grows from a unique initial seed. Moreover, fluctuations were observed even when carefully selecting crystals grown from a single seed.[13] This raises new questions. Is a "fixed point" of final enantiomeric excess really reached? And if it is really reached, how can such a partial homochiral state be explained, with its observed fluctuations? Previous models gave a predictable final value for the ee with no fluctuations. We therefore extended the previous model to include the effects of homogeneities more realistically.

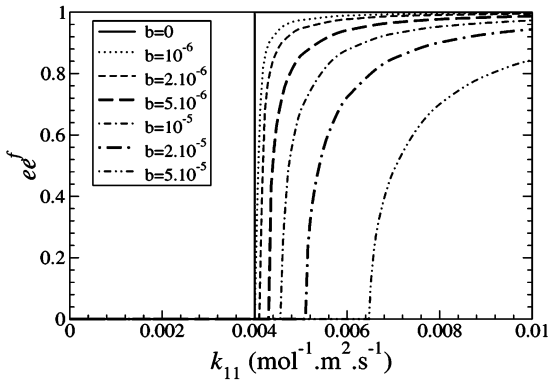

Figure 1. Bifurcation diagram of homogeneous models. The absolute value of the enantiomeric excess of the stable fixed point is given as a function of k_{11}. Several models were simulated, characterized by the parameter b, with $k_{13} = b$ mol^{-1}·m^2·s^{-1} and $k_{02} = b$ s^{-1}. Fixed parameters: $k_{01} = 0.001$ s^{-1}, $k_{12} = 0.002$ mol^{-1}·m^2·s^{-1}, $k_{20} = 0.005$ s^{-1}.

Imperfect Selectivity in the Homogeneous Kinetic Model

In the previous model,[11] a major difference appeared with the experiments: the nonracemic states are always totally homochiral, and the bifurcation pattern is discontinuous (the stable ee being 0 below the critical point, and 1 above it). Such a "hard transition" was observed in another symmetry breaking system,[8] where it was shown that such an uncommon behavior is actually only observed in the most extreme models, which can be analytically solved, when some kinetic parameters are set to zero. This implies totally selective reactions, only allowing either totally racemic or totally homochiral states as possible fixed-point or final states. In the previous study[11] it was assumed that the rate constants k_{13} and k_{02} were negligible and were set equal to zero. To check if this assumption caused the discontinuous transition, kinetic equations based on the model shown in Scheme 1 (the same equations used in ref 11) were studied, this time by adding nonzero parameters for the k_{13} and k_{02} parameters. Numeric integrations were performed, using a fourth-order Runge−Kutta with an adaptative step-size algorithm.[14] The XPPaut software was used.[15]

The bifurcation diagrams were calculated for a given set of parameters ($k_{01} = 0.001$ s^{-1}, $k_{12} = 0.002$ mol^{-1}·m^2·s^{-1}, and $k_{20} = 0.005$ s^{-1}) as a function of k_{11}, for several values of k_{13} and k_{02}. For the sake of simplicity, the numerical values of these two rate constants were set equal to a parameter b (parameter b in Figure 1). The discontinuous pattern is observed when $b = 0$, while a more classical diagram is observed in all other cases, with a continuous increase of the absolute value of the enantiomeric excess of the stable fixed point from 0 to 1 after the bifurcation point. When k_{13} and k_{02} values increase, the critical value of k_{11} increases, and the maximum value of the enantiomeric excesses of the fixed points decreases (see Figure 1). This result sheds some light on the partial homochirality reached by experimental binaphthyl crystallizations, suggesting that the kinetic rates k_{13} and k_{02} are not negligible in these systems.

Three-Dimensional Kinetic Model

The homogeneous description of the last model may not precisely describe the reality, as most species are actually in a fixed environment. The homogeneous kinetic description as-

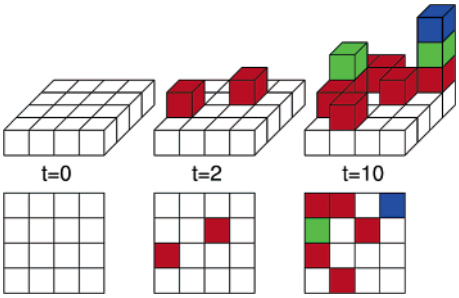

Figure 2. Representation of a stochastic crystal growth on a 4 × 4 layer as a function of time: first row, three-dimensional representation; second row, upper view of the surface. The time is given as the number of elementary stochastic steps. White boxes represent layer 0, red layer 1, green layer 2, and blue layer 3. New growth units can be attached on the top of other growth units, so that there are always the same number of reactive sites (the one seen in the upper view).

sumes that the probability of meeting of two compounds is proportional to their respective concentration. This would imply either that the compounds are able to diffuse quickly on the surface, or that their homogeneous distribution inside the system is somehow fixed. As a typical example, the description of the reactions of rate k_{12}—involving induction of homochirality by either lateral or interfacial subunits of opposite configuration—will not be accurate if the system is composed of several large homochiral blocks: these reactions can actually only occur in the interface between the homochiral blocks. The number of possible events is thus much lower than in the case of homogeneous distribution. The corresponding global kinetic rate will then be lower than expected. These limitations can be taken into account in a system describing the environment of each growing subunit as described by Saito et al.[10]

Moreover, this leads us to consider a discrete description of the system, rather than a continuous homogeneous system. It has been reported that such a discrete microscopic description of complex dynamic systems can explain macroscopic behavior that cannot be predicted by uniform continuous models.[16] In this case, statistical fluctuations are inherently taken into account, which is of great importance here.

Description of the Model. A new three-dimensional model has thus been built, on the basis of the reaction Scheme 1 used in the homogeneous model. In this model, the description of the whole crystal is in terms of minimal growth subunits as building blocks, each one being individually described, in relation to its own environment. For the sake of simplicity, a cubic arrangement was assumed, so that each elementary growth subunit can be localized by integer orthogonal coordinates. To avoid edge effects, an euclidean torus geometry was introduced (i.e., each opposite side of the whole system is connected). The nonlinear induction (reactions k_{11}, k_{12}, and k_{13}) can now be directly described by the induction of the configuration of a C, I, or G elementary growth subunit that is directly in lateral contact with a reacting L.

The reaction starts on top of a preexisting planar layer (that can be either racemic or homochiral). Any new subunit can be attached on top of another existing interfacial subunit, following local stochastic rules, that is each site has a specific probability of reaction depending on the respective environment. Thus, the crystal is being progressively built by a vertical addition of crystal subunits. A graphical representation of this process is given in Figure 2. Every new subunit becomes first a growth subunit that can react to become a new interfacial subunit (and thus becomes one new site of nucleation). As a consequence, the reactive layer is of constant dimension, with always one reactive site at each place on the crystal surface.

The stochastic rules imply that new elements are added randomly on the surface, and thus that the surface may not grow very regularly. However, lateral subunits act as catalysts, so that the probability for the addition of a subunit is higher in hollows that that on peaks. Globally, a quite homogeneous vertical growth is thus generally obtained, with a more or less important roughness.

Computer Modeling. A discrete stochastic description of the system has been used.[17] Each elementary growth subunit is supposed attached to one element of a three-dimensional matrix, and no diffusion is assumed to occur (this is actually not a real limitation, as solid compounds cannot diffuse, and as all liquid compounds are identical). All compounds that can react at a given time t are listed. They can either be an L subunit (liquid subunit, being on top of an interfacial (I) crystalline subunit) or G compounds (growth layer subunit, waiting to become part of the crystal (C) phase). The probability of each one of these subunits being transformed into another one is calculated on the basis of the corresponding stochastic kinetic rates, and of their respective environment: the four lateral subunits (which can catalyze and induce crystallizations) and the surface subunit on which the added subunit sits.

The stochastic rate p is defined by the probability of occurrence of a given elementary reaction, per unit of time. In the case of first-order (k_{20}) and pseudo-first-order (k_{01} and k_{02}) reactions, stochastic rates and kinetic (macroscopic) rates are equals. They are expressed in s^{-1}. In the case of pseudo-second-order reactions occurring on a uniformly distributed surface (k_{11}, k_{12}, and k_{13}), the relationship is $k_x = 4Sp_x$. S is the molar surface of the crystal (i.e., the surface occupied by 1 mole of growing subunits). The coefficient 4 accounts for the four possibilities of induction at a given site by each one of its lateral neighbors. The total sum of all stochastic rates of all possible events in the system at a given time (δp) is calculated, and a random number is drawn from the uniformly distributed interval $[0,\delta p[$. This number allows one to choose which event will actually happen in the infinitesimal time $\delta t = 1/\delta p$.[18]

The interest of such an algorithm is to inherently take into account the statistical fluctuations (see the Supporting Information) and to keep the microscopic description. On top of that, all stochastic rates are in the same unit (s^{-1})—as representing directly a probability of reaction rather than a macroscopic kinetic rates—which allows their direct comparison.

System Behavior. Simulations were performed for a wide range of parameters. Several types of states and behavior were observed. They could be classified in the following six categories (see Figure 3):

Racemic state: For certain values of the system parameters, subunits of both enantio-configurations exist in the crystal in roughly the same quantity, and are distributed uniformly on the surface, with no apparent structure. This corresponds to the simple case of a racemic crystal. Fluctuations of the enantiomeric excess around zero are as predicted by statistical laws[18] (in the case of a surface containing 256^2 elementary growth subunits, statistical fluctuations of the enantiomeric excess equal about $1/256 = 4 \times 10^{-3}$).

Homochiral state: A racemic state can become unstable and make a transition to a predominantly homochiral state. The elementary growth subunits of the opposite configuration are uniformly distributed on the surface as very small clusters.

These first two cases are the only ones that could be predicted and described in the homogeneous model. It should be noticed that in contrast to what could be previously described, the evolution from an unstable racemic state toward a stable

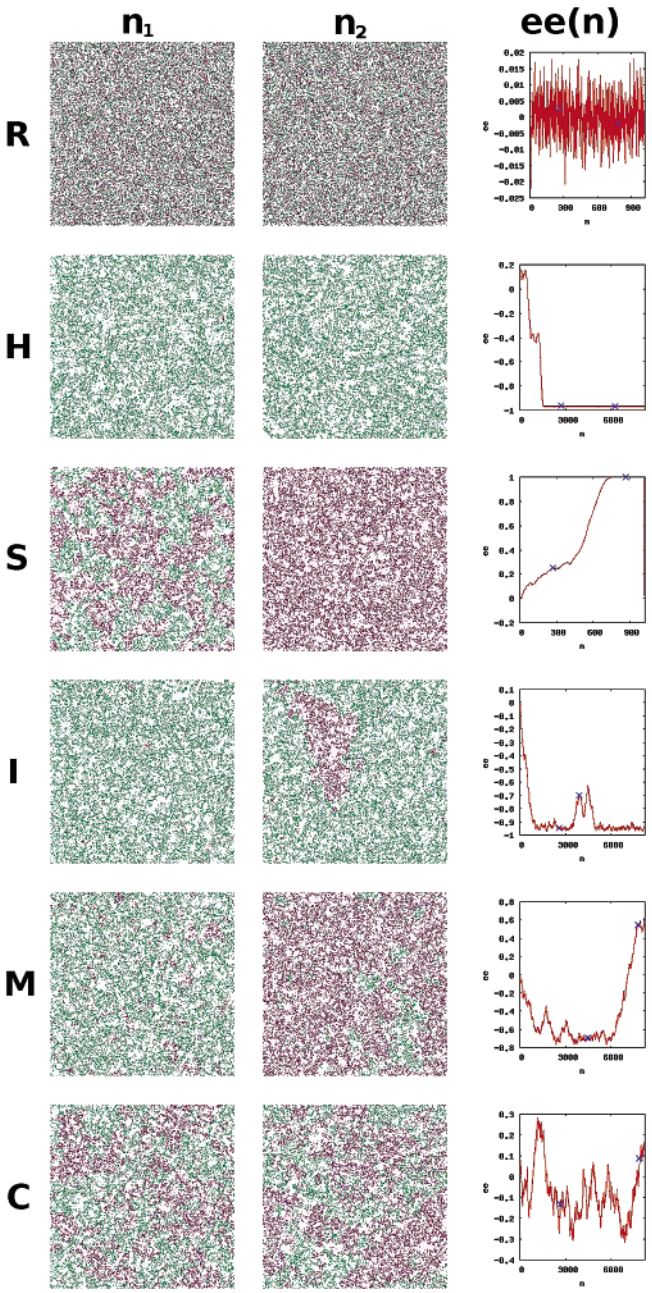

Figure 3. System behavior: R, racemic; H, homochiral; S, structured; I, local instabilities; M, multistabilities; C; chaotic. The two first columns indicate the state of the surface of the crystals when the crystallization front growths reached layers n_1 and n_2: light red, I_R; light green, I_S; dark red, G_R; dark green, G_S. The third column indicates the enantiomeric excess of each layer of the crystal. The blue crosses indicates the positions of layers n_1 and n_2: R, $n_1 = 256$ and $n_2 = 768$; H, $n_1 = 2688$ and $n_2 = 6208$; S, $n_1 = 264$ and $n_2 = 872$; I, $n_1 = 2624$ and $n_2 = 3904$; M, $n_1 = 4480$ and $n_2 = 7808$; C, $n_1 = 2688$ and $n_2 = 7872$.

homochiral state can be nonmonotone, presenting some oscillations or fluctuations before reaching a stable steady state.

Transient structures: In most simulations, structures with "stripes" can be noticed. They are generally transitional structures, allowing the evolution from an initially random distribution to a stable homochiral state. In some cases, such structures may seem stable, but they are actually related to very slowly evolving patterns that are correlated with a very irregular surface and a mainly vertical crystal growth (i.e., presenting scarce lateral induction and strong surface induction, leading to a high conservation of the underlying structures).

Local instabilities: Some partially homochiral systems can present some intrinsic local instabilities. The system can stay a long time in a roughly stable state, with a constant value of ee, and then quickly change to a state with low ee. This behavior is correlated with the onset of a large embedded homochiral block of opposite configuration than the major part of the crystal surface. This corresponds to a local inversion of the enantiomeric excess inside a limited spatial area, that consequently implies the global decrease of the enantiomeric excess. Such structure is, however, very unstable, and disappears as quickly as it appeared.

Multistable state: These states are quite similar to the preceding ones, but the instabilities have much more dramatic consequences: fast ee variations lead not only to unstable transient formation of embedded structures of opposite configuration, but also to total and fast inversion of the whole system to the opposite configuration.

Chaotic behavior: In some cases, no stability is reached. Huge variations of ee (much higher than purely statistic fluctuations) and structures are observed. They are totally random, and no specific structure can be identified.

Embedded Structure Formation. *3D Representation of Embedded Structures.*The organization of homochiral substructures within the crystal phase has been more precisely studied. A first simple three-dimensional representation has been drawn for typical crystals (quasihomochiral, with local instabilities, and chaos) by plotting surfaces at the interfaces between crystals of opposite configuration in a three-dimensional representation (see Figure 4).

In quasihomochiral systems (Figure 4A), there are several small crystals of opposed configuration embedded in the matrix, with a uniform distribution. When local instabilities occur (Figure 4B), these inclusions are in greater number, and are larger. When the system is chaotic (Figure 4C), all the structures are merged in a unique spongelike structure.

Repartition of Structure Sizes for All System Types. For several simulations, and for each kind of system, all the homochiral substructures present in the whole three-dimensional medium were listed and classified according to their size s (i.e., the number of elementary subunits they contain). The total number of substructures $n_t(l,m)$ whose size s is so that $l \times 10^m \leq s < (l+1) \times 10^m$ was determined for $1 \leq l \leq 9$ and $0 \leq m \leq 6$, with l, s, and m all being integer values. $n_t(l,m)$ corresponds to the total number of substructures of average size $s = (l + {}^1/_2) \times 10^m$. The average number $n(s)$ of substructures of average size s could then be determined by $n(s) = n_t(l,m)/10^m$. The computed values where then drawn, plotting $\ln(s)$ as a function of $\ln(n(s))$ (see Figure 5). In these graphs, a linear evolution of slope p would correspond to a variation of $n(s)$ proportional to s^p. In all cases, a very regular distribution is observed, even for very large fluctuations and chaotic systems:

Homochiral type: The subunits of the major configuration are all fused in a one-block matrix, in which are embedded crystallites of the opposite configuration. The slope of their evolution is initially slow (-1.5) but quickly increase (up to -5). This means that the major part of the embedded crystals are small, and that larger ones become quickly scarce.

Local instabilities type: When local instabilities begin to occur, the subunits of the major configuration are still mainly fused in a unique matrix. An important change is observed for the distribution of embedded structures. The curve becomes composed mainly of two linear parts. At first (up to structures of about 20 elementary subunits) a slope of -1.5 is observed and then the slope changes to only -2. This means that

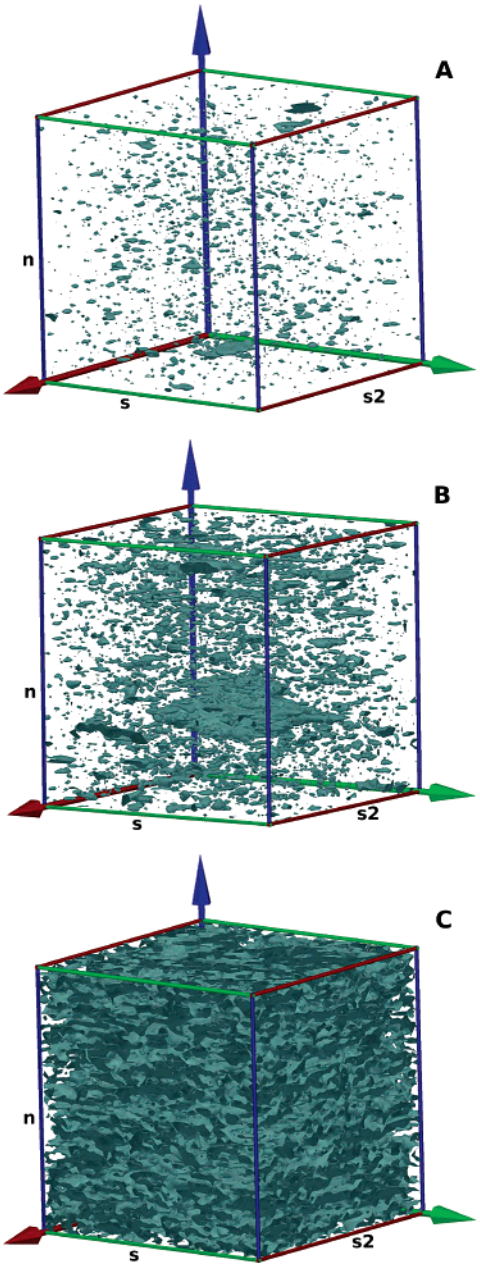

Figure 4. Embedded structure representations. The interface between crystals of opposite configuration is represented by the green surfaces: A, partially homochiral system; B, local instabilities; C, chaotic system. s and s_2 represent the horizontal dimension of the crystal surface, and n is the number of layers. These graphs were drawn from raw data with use of IFRIT software[19] and the VTK library.[20]

structures of size up to 20 become quite common, and that larger structures are far less scarce (distribution in $1/s^2$ rather than $1/s^5$). As a consequence, embedded structures containing several thousands of subunits begin to appear. Small inclusion of the major configuration also begins to be detected. This corresponds to substructures embedded in the larger structures. They are more scarce than the others, but their distribution is similar (slope of -2).

Chaotic type: When the chaotic state is reached, both configurations behave in the same manner. There is, at this point, two major large, and interleaved, structures. As a consequence, the number of independent inclusions is lower, and the larger one disappears as they are merged into a unique structure. A two-mode size distribution is still observed (initial slope of about -2, which increases for larger structures to -3).

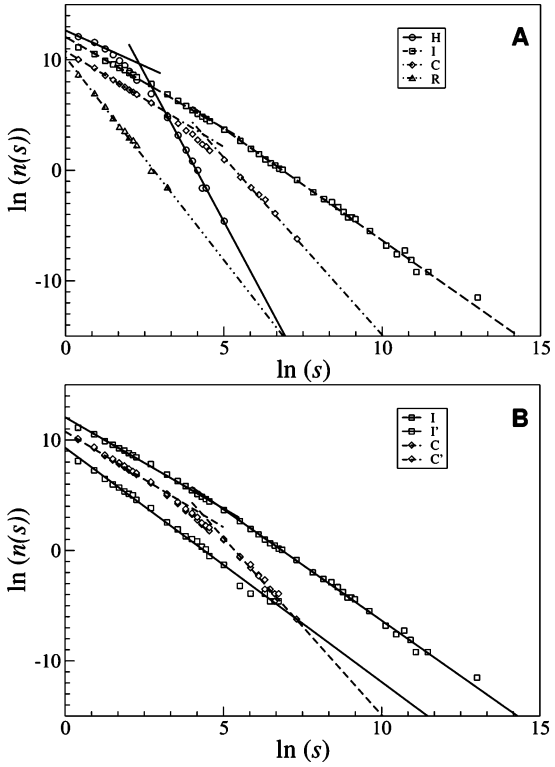

Figure 5. Structure size distribution of embedded structures. Size of the inclusions of the minor configuration (A): H, partially homochiral system; I, local instabilities; C, chaotic system; R, racemic system. Size of the inclusions of both configurations (B): I, local instabilities (minor configuration); I′, local instabilities (major configuration); C and C′, chaotic system (both configurations present in the same amount).

Racemic type: When the system is racemic, the two major structures are preponderant and more intertwined, while embedded substructures become very scarce.

Some additional simulations were performed with variations of the run length (vertical homogeneity) and the surface size (horizontal homogeneity). A very good reproducibility could be observed, showing a good uniformity of the distribution of the inclusions inside the whole crystal.

Interpretation. From our computer simulation we conclude that in the homochiral state, there are small inclusions of the opposite configuration. The statistical distribution is shifted to the small sizes (i.e., the larger ones become quickly scarce). As the bifurcation point is approached, the large sizes became more frequent. The following random burst of large instabilities still follows a regular statistical distribution; these represent the well-known critical fluctuations near an instability. It can be interpreted that when inclusions became more frequent and larger, they came closer to each other. Thus, the probability to fuse themselves into a larger inclusion increases, explaining the increase of the probability of larger structures. At one point, the sizes and frequencies of inclusions increase enough so that we observe the onset of two large interconnected matrixes of both configuration, occupying the whole crystals in two interwoven spongelike structures: the system is chaotic. Then, going further from the bifurcation point, the number of independent inclusions keeps decreasing, letting the spongelike structures become predominant. Their "pore" size also keeps decreasing, so that the distribution of elementary growth subunits of both configurations became very random.

Bifurcation Diagram. A systematic study was performed, varying parameter $p_{12} \in [1,6]$ (in s^{-1}). Other parameters were fixed to $p_{01} = 0.1\ s^{-1}$, $p_{20} = 10\ s^{-1}$, $p_{11} = 10\ s^{-1}$, and $p_{02} =$

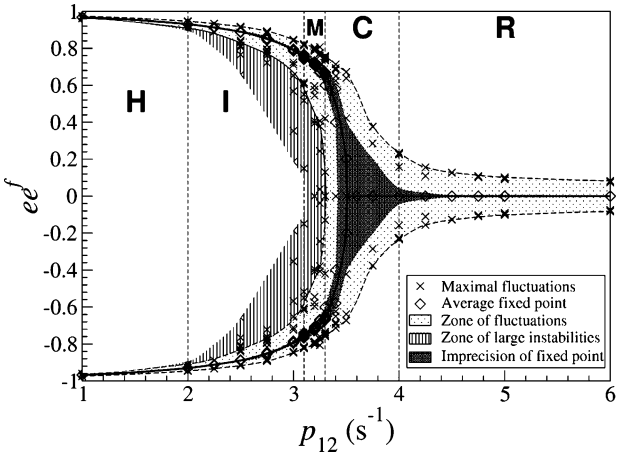

Figure 6. Bifurcation diagram of the three-dimensional system. The circles indicate the average value of the fixed point. The gray zone gives the minimal and maximal value of the average value of the enantiomeric excess of the fixed point when computed on 100 successive layers anywhere in the crystal (large difference indicates chaotic systems). The dotted zone indicates the maximal fluctuations around the fixed point, not taking into account local instabilities. The striped zone gives the maximal fluctuations around the fixed point, taking into account local instabilities. The five behavior zones are indicated by the letters H, I, M, C, and R as defined in Figure 5.

$p_{13} = 0.01\ s^{-1}$. The system then continuously evolves from a homochiral state (low values of p_{12}) to a racemic state (high values of p_{12})—successively passing through local instabilities, multistabilities, and chaotic states—describing a bifurcation pattern (see Figure 6). For low values of p_{12}, the steady state is homochiral. When p_{12} is progressively increased, local instabilities begin to occur. The intensity and the frequency of these instabilities increases with p_{12}, until the point where they are greater than the absolute value of the ee of the steady state. At this point, the instabilities can cause the system to flip from one configuration to the other. These changes of configuration get more frequent when approaching the bifurcation point, until the point that no real steady state can be observed and the ee becomes chaotic. This is the state at which the system is beginning to lose its stability; it exhibits the well-known critical fluctuations. The absolute value of these variations is then slowly decreasing with p_{12}, until the point that they are of the same order as the statistical fluctuations. The system is then in a stable racemic fixed point.

This bifurcation pattern is very similar to that of the homogeneous model, but only statistically. While the average ee follows the bifurcation diagram predicted by the homogeneous model, our model gives us a more detailed picture of how the fluctuations evolve as the system passes through the bifurcation point. We can clearly see the so-called critical fluctuations that are expected to arise near a transition point—critical opalescence being an example.

Conclusion

A first extension of the homogeneous model has shown that the introduction of imperfect selectivity of reaction (by nonzero kinetic rates for k_{13} and k_{02} parameters) can explain the onset of partial homochirality. Even when starting from a single seed, crystals of opposite configuration can be formed through imperfect induction. Our simulation shows that the assumption of perfect selection (the assumption that $k_{13} = k_{02} = 0$) gives rise to a "hard transition", which is more like a first-order phase transition.

While the homogeneous analysis could predict the presence of the bifurcation point, the three-dimensional approach could describe that local instabilities can inherently exist in the system, inclusion of opposite configuration being stable. Because of the spatial distribution of growing subunits on the surface of the crystal, inhomogeneities occur but the growth kinetics favor the merging of the substructures of the same chirality into homochiral substructures. This can be characterized by more or less large fluctuations of the final enantiomeric excess (ee) in the crystal phase, particularly when the system is near the bifurcation point. Depending on the values of the crystal kinetic parameters, which depend on the chiral interaction energies between the R and S subunits, each crystallizing system can exhibit large or small fluctuations in the ee of a crystal. This can explain the experimental fluctuations of the ee of the crystal. In these cases, crystals of opposite configuration can easily be formed within a homochiral crystal. The fixed point is thus only statistically reached. The fact that experiments show low ee (60%) and large fluctuations, even when crystallizations are very carefully driven, when only one crystal has nucleated should indicate that the binaphthyl system is probably not far from its bifurcation point, implying the possibility to observe fluctuations of the enantiomeric excess.

The introduction of a nonhomogeneous description of dynamical systems with an unstable racemic state brings additional pieces of information. Qualitatively, some complex states can actually exist close to the bifurcation point (local instabilities, chaotic states) or transiently (temporary Turing-like patterns when evolving from a racemic to a homochiral state). Moreover, these phenomena can be quantitatively correlated to some experimental observations, as shown for the example of 1,1′-binaphthyl crystallization. Finally, even if fluctuations can be observed, the fixed point is always—at least statistically—reached. As a consequence, even if ee of opposite sign emerges in different places on a system, one single configuration can predominate on the whole system when the system is far enough from the bifurcation point.

Acknowledgment. We are thankful for a Postdoctoral Fellowship for Foreign Researchers (P 04804), Grant-in-Aid for JSPS Postdoctoral Fellows (16-04804(X50079)), and Grant-in-Aid for Scientific Research (C) (17540361) from the Japan Society for Promotion of Science for supporting this work. We also are grateful to the Grant-in-Aid for the 21st Century COE program "Keio Life Conjugate Chemistry" from the Ministry of Education, Culture, Sports, Science, and Technology, Japan.

Supporting Information Available: Description and source code of the computer program of the three-dimensional stochastic simulation; mathematical relationship between stochastic kinetic rates and macroscopic kinetic rates; mathematical calculation of statistical fluctuations of the enantiomeric excess; and GIF animations of the crystallization processes for the different types of system behavior. This material is available free of charge via the Internet at http://pubs.acs.org.

References and Notes

(1) Hicks, J. M., Ed. *Chirality*: *Physical Chemistry*; ACS Symposium Series No. 810; American Chemical Society: Washington, DC, 2002.

(2) Curie, P. *J. Phys.* **1894**, *3*, 393−417.

(3) (a) Kondepudi, D. K.; Nelson, G. W. *Phys. A* (*Amsterdam, Neth.*) **1984**, *125*, 465−496. (b) Kondepudi, D. K.; Nelson, G. W. *Nature* **1985**, *314*, 438−441.

(4) Frank, F. C. *Biochim. Biophys. Acta* **1953**, *11*, 459−463.

(5) (a) Kondepudi, D. K.; Kaufman, R. J.; Singh, N. *Science* **1990**, *250*, 975−976. (b) Kondepudi, D. K.; Bullock, K.; Digits, J.; Hall, J. K.;

Miller, J. M. *J. Am. Chem. Soc.* **1993**, *115*, 10211−10216. (c) Buhse, T.; Durand, D.; Kondepudi, D. K.; Laudadio, J.; Spilker, S. *Phys. Rev. Lett.* **2000**, *84*, 4405−4408. (d) Viedma, C. *Phys. Rev. Lett.* **2005**, *94*, 065504-(1−4).

(6) (a) Kondepudi, D. K.; Laudadio, J.; Asakura, K. *J. Am. Chem. Soc.* **1999**, *121*, 1448−1451. (b) Asakura, K.; Soga, T.; Uchida, T. *Chirality* **2002**, *14*, 85−89. (c) Asakura, K.; Nagasaka, Y.; Hidaka, M.; Hayashi, M.; Osanai, S.; Kondepudi, D. K. *Chirality* **2004**, *16*, 131−136.

(7) Kondepudi, D. K.; Asakura, K. *Acc. Chem. Res.* **2001**, *34*, 946−954.

(8) Plasson, R.; Bersini, H.; Commeyras, A. *Proc. Natl. Acad. Sci. U.S.A.* **2004**, *101*, 16733−16738.

(9) (a) Epstein, I. R.; Showalter, K. *J. Phys. Chem.* **1996**, *100*, 13132−13147. (b) Epstein, I.; Pojman, J. *An Introduction to Nonlinear Chemical Dynamics*; Oxford University Press: New York, 1998

(10) (a) Zel'dovich, Ya. B.; Mikhailov, A. S. *Sov. Phys. Usp.* **1987**, *30*, 977−992. (b) Saito, Y.; Hyuga, H. *J. Phys. Chem. Jpn.* **2004**, *73*, 1685−1688.

(11) Asakura, K.; Nagasaka, Y.; Osanai, S.; Kondepudi, D. K. *J. Phys. Chem. B* **2005**, *109*, 1586−1592.

(12) Randolph, A. D.; Larson, M. D. *Theory of Particulate Processes*, 2nd ed.; Academic Press: San Diego, CA, 1991.

(13) Asakura, K.; Soga, T.; Uchida, T.; Osanai, S.; Kondepudi, D. K. *Chirality* **2002**, *14*, 85−89.

(14) Kaps, P.; Rentrop, P. *Numer. Math.* **1979,** *33*, 55−68.

(15) Web site: http://www.math.pitt.edu/∼bard/xpp/xpp.html.

(16) Shnerb, N. M.; Louzoun, Y.; Bettelheim, E.; Solomon, S. *Proc. Natl. Acad. Sci. U.S.A.* **2000**, *97*, 10322−10324.

(17) Lukkien, J. J.; Segers, J. P. L.; Hilbers, P. A. J. *Phys. Rev. E* **1998**, *58*, 2598−2613.

(18) See the Supporting Information for more details.

(19) Web site: http://casa.colorado.edu/∼gnedin/IFRIT.

(20) Web site: http://public.kitware.com/VTK.